Competition between Na^+ and Rb^+ in the minor groove of DNA

X. Shen,[1,2] N. A. Atamas,[3] and F. S. Zhang[1,2,4,*]

[1]*Key Laboratory of Beam Technology and Material Modification of Ministry of Education, College of Nuclear Science and Technology, Beijing Normal University, Beijing 100875, China*

[2]*Beijing Radiation Center, Beijing 100875, China*

[3]*Physics Department, Taras Shevchenko Kyiv National University, Kyiv 03022, Ukraine*

[4]*Center of Theoretical Nuclear Physics, National Laboratory of Heavy Ion Accelerator of Lanzhou, Lanzhou 730000, China*

(Received 10 January 2012; published 22 May 2012)

The competition between Na^+ and Rb^+ ions in the minor groove of a synthetic B-DNA dodecamer d (CGCGAATTCGCG) is studied using molecular dynamics simulations as the ratio of these two ions changing from 9:1 to 1:9 with the DNA merged into the solvent of water molecule at 298 K. When the concentration of Rb^+ ions increases, from minority to majority, Na^+ ions are gradually released from the A tract, and the binding sites in the minor groove are occupied by Rb^+ ions, extending from the A tract to the whole minor groove. Comparing Na^+ with Rb^+ ions, the conformation of the minor groove is influenced strongly by Na^+ ions.

DOI: 10.1103/PhysRevE.85.051913 PACS number(s): 87.14.gk, 87.15.H−, 61.25.Em

I. INTRODUCTION

For the storing, duplication, realization, and transcription of the genetic information, DNA is a hopeful fundamental building block in the fields of biochemistry, nanotechnology, and molecular computing [1–4]. The minor groove of DNA plays a crucial role in the process of protein-DNA docking. In turn, it is affected by the presence and interactions with external environments factors, such as water molecules [5,6] and groove-bound ions [7,8]. The cations (such as spermine and spermidine) [9] provide a stabilizing medium for the maintenance of the highly compact and organized DNA secondary structure [10]. They reside in the minor groove, form-specific ion-DNA interaction and influence the stability and dynamics of the minor groove [11,12]. Therefore, it is important to study the mechanisms and the properties of the minor groove in ionic solutions, such as DNA-cation electrostatic interaction, the activity of water molecules on the hydrophobic DNA surface, base stacking, and hydrogen bonds [13–17].

The physicochemical properties of different alkali-metal ions in the minor groove of B-DNA have long been studied by numerous experimental and theoretical evidence, in which Na^+ and K^+ ions are known to play important roles in the stabilization and structural polymorphism (such as A-DNA, B-DNA, Z-DNA, *etc*.) of DNA [18–24]. Stellwagen *et al*. [22] provided evidence of Na^+ ions residing in the minor groove by capillary electrophoresis experiments. Young *et al*. [23] proposed that the strongly electronegative pockets in the Dickerson-Drew dodecamer (DDD) harbor Na^+ ions, which intrude into the "spine of hydration" in the minor groove and remain at the A tract with fractional occupancies. Cheng *et al*. [24] found Na^+ ions prefer to interact with phosphate group while K^+ ions bind to the electronegative sites of DNA bases in the minor grooves. The ion distributions in the minor groove are affected by the increasing number of the solvent.

Those studies show that Na^+ and K^+ ions interact preferentially with different DNA sites [23,24]. However, Na^+ and K^+ ions (atomic number is smaller than Rb^+ and Cs^+ ions in the alkali metals, written as the lighter ions in the following) are difficult to distinguish from water molecules in the experiments for the limited resolution of DDD crystal structures. Thus Rb^+ and Cs^+ ions (written as the heavier cations in the following) are employed, and the partially occupied ion sites have been reliably detected [18,25,26]. Tereshko *et al*. [25] crystallized the DDD sequence in the presence of Rb^+ or Na^+ ions and found the ions are more optimally suited to replace the water of the inner spine than Na^+ ions. Woods *et al*. [26] also estimated Cs^+ ions' occupancy within hybrid solvent sites at the A tract of the minor groove.

Since different cations have different effects in maintaining higher-order chromatin structure, it is important to consider the competition of the distribution of two cations around DNA. Several experiments reported the competition between monovalent cations [18,27–29], divalent ions [30,31], and even ammonium ions [27]. Ida *et al*. [18] directly measured the competitive Rb^+ and Na^+ binding to the G-quadruplex channel site. Denisov *et al*. [27] indicated that heavier alkali-metal ions bind to the minor groove with similar affinity as Na^+ ions, whereas ammonium ions' binding is somewhat stronger. Marincola *et al*. [28] extended the previous magnetic relaxation dispersion studies and focused on the competition between Na^+ and Rb^+ ions in a high purity of DNA. They measured the full Na^+ and Rb^+ profiles in DNA solutions and suggested that groove-bound ions significantly influence the energetics and structural polymorphism of DNA and demonstrated that the affinity of Rb^+ ions is higher than that of Na^+ with DNA. Savelyev *et al*. [29] compared the systems mixing Na^+ and K^+ ions with and without Cl^- using molecular dynamics (MD) simulations. Their results suggested that Na^+ ions condense more strongly around DNA in both situations, and K^+-Cl^- clustering effect screens K^+ ions from DNA electrostatic field.

The systems containing both Na^+ and Rb^+ ions are performed with MD, and MD simulations can show some interesting and subtle results that cannot be present by experiments [28], for example, the detailed distribution of ions around the atoms of DNA in the minor groove in the

*Corresponding author: fszhang@bnu.edu.cn

competition of ions. There still are two questions that the experiments and theories did not answer: (1) the relationship of the A tract and G tract in the competitions and (2) can cation binding induce the structural adjustment in DNA, or can this structural feature be a preexisting intrinsic property of DNA favoring cation binding [32,33]. However, few studies focus on DNA structure changes accompanied by the competition of ions. By varying the ratio of Na^+ and Rb^+ ions, we study how the competition happens between these two kinds of ions in the minor groove and try to catch the mechanisms behind. The very exact binding sites in the minor groove are provided at atomic scales, which are shown by microscope images [e.g., spatial distribution functions (SDFs)]. The radial distribution functions (RDFs) of the cations and solvent with DNA present the distinct ion-DNA interaction strength, the permeating order of two ions, and the behaviors of Na^+ and Rb^+ ions residing at the A tract and G tract. The change of local DNA conformation (here we focus on the width and depth of the minor groove) is studied to investigate the relationship between the concentration of each ion with the extent of the conformation changing.

In this work, we compare the affinity of Na^+ and Rb^+ ions in the minor groove of DNA and study the competition between these two cations as the ratio of these two ions changing from 9:1 to 1:9. After the introduction, we explain the model of the solvent molecule, the DNA segment and ions, and the simulation method in Sec. II. In Sec. III our results demonstrate that the G tract is like the "springboard" for the ions "jumping into" the A tract with the changing of width and depth of the minor groove. The conclusion is presented at the end of the paper.

II. THEORY AND SIMULATION DETAILS

The NMR structure of a synthetic B form duplex d (CGCGAATTCGCG) named 171d is chosen from the Protein Data Bank (PDB) [34] as the starting structure in each simulation. The 171d duplex is extensively studied because of its biological importance. It contains the recognition site of the *Eco*RI restriction enzyme and is frequently used in gene recombination techniques. The force-field parameters of Na^+, Rb^+, and Cl^- ions are selected as $\varepsilon_{Na^+} = 0.358$ kJ/mol, $\sigma_{Na^+} = 2.73$ Å, $\varepsilon_{Rb^+} = 1.602$ kJ/mol, $\sigma_{Rb^+} = 3.57$ Å, and $\varepsilon_{Cl^-} = 0.168$ kJ/mol, $\sigma_{Cl^+} = 4.86$ Å [35], respectively. The model solvent is derived from the widely used flexible simple point charge (SPC) water molecule model.

The intermolecular energy consists of two parts: $E = E_{LJ} + E_C$, where E_{LJ} is the Lennard-Jones interaction and E_C is the Coulomb interaction. They are expressed as

$$E_{LJ} = 4\varepsilon_{ij}\left[\left(\frac{\sigma_{ij}}{r_{ij}}\right)^{12} - \left(\frac{\sigma_{ij}}{r_{ij}}\right)^{6}\right], \quad (1)$$

$$E_C = \frac{q_i q_j}{4\pi\varepsilon_0 r_{ij}}, \quad (2)$$

where ε_0 is the vacuum permittivity and r_{ij} presents the distance between two atoms. In Lennard-Jones interaction, the first term is the short-range repulsion for molecules or atoms being too close to each other, and the attraction owing to the dispersion forces is described in the second term. The Coulomb interactions between point charges describe the hydrogen bond and give the local orientational structure [36,37]. Comparing with E_C, E_{LJ} contributes only 1% of the E. The force field of Cornell *et al*. [38] is implemented with Amber 94 parameters, including hydrogen bonds between base pairs, for their special accuracy in reflecting the effects of water activity [39]. The flexibility of SPC model is considered with a Morse type of potential for its covalent bonds [40].

The M.DynaMix packages, which are developed for simulations of arbitrary mixtures of molecules and macromolecules in solutions, are use to perform MD [41,42]. The double time-step algorithm by Tuckerman *et al*. [43] is implemented, and the short time step is 0.2 fs for the fast nearest short-range (within 4.8 Å) interactions, while the long time step for those more slowly fluctuating interaction is 2.0 fs. The Ewald sum method is used to treat the electrostatic interactions with screening parameter α taken as $\alpha = 3/R_{cut}$ and the reciprocal space cutoff determined [44] by $\exp(-\pi^2 k_{max}^2/\alpha^2) = \exp(-9)$. The cutoff for this long-range interaction is 14 Å.

There is one 171d DNA segment, 3600 SPC solvent molecules and 200 mixed cations in each periodic hexagonal cell ($48 \times 48 \times 56$ Å^3). Two hundred mixed cations are added in as well as 178 Cl^- co-ions with the relative ratio of Na^+ and Rb^+ ions changing from 9:1 to 1:9, as (1) 180 Na^+ and 20 Rb^+ (abbreviated as Na180Rb20), (2) 150 Na^+ and 50 Rb^+ (Na150Rb50), (3) 100 Na^+ and 100 Rb^+ (Na100Rb100), (4) 50 Na^+ and 150 Rb^+ (Na50Rb150), (5) 20 Na^+ and 180 Rb^+ (Na20Rb180). Five simulations are carried out in the NVT ensemble [45] at 298 K. At the beginning, DNA is fixed in the box center along the Z direction, and a 1 ns NVT simulation is performed to allow the solvent molecules and ions to form the outer shells around DNA obtaining the preliminary balance. Then all freedom degrees are released in a following 1 ns NVT running to produce equilibrium of the system. After that, the following simulations of 60 ns are carried out for dynamics and structure analyses. The structure parameters are analyzed by the program Curves [46–49] continually for the precise values (the width and depth of the minor groove are defined in detail in Ref. [46]).

III. RESULTS AND DISCUSSION

The convergence of cations around DNA is examined by ion occupancies with each atom of the segment. Occupancy here is defined as the integration of the first maximum of the corresponding RDF within the primary layer of the solvent. Figure 1 shows occupancies of Na^+ and Rb^+ ions with atoms of the inner eight base pairs along the strands form 5′ to 3′ in Na100Rb100. For one strand, the occupancies are plotted at a positive direction; for another strand the occupancies are plotted at a negative direction. The perfect symmetry with respect to the horizontal is almost achieved for Na^+ ions, and the palindromic symmetry for Rb^+ ions is appeared to some extent in the trajectory, similar with the calculations of Ponomarev *et al*. [50]. It seems that both ions are converged around DNA, and the simulations are equilibrated with respect to ion distributions. However, the ion convergence has been influenced by the competitive of Na^+ and Rb^+ ions. The global occupancies of Rb^+ ions are larger than that of Na^+ ions, indicating that Rb^+ ions prefer to bind with the DNA.

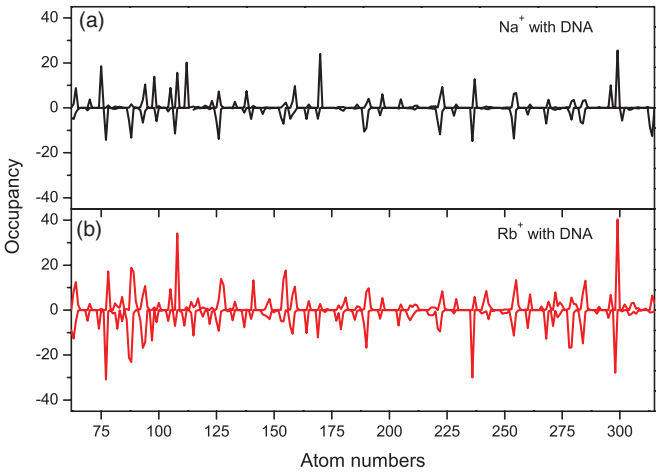

FIG. 1. (Color online) The average ion occupancies for Na^+ (a) and Rb^+ (b) ions with each DNA atom of the inner eight base pairs along two strands d (CGCGAATTCGCG) from 5′ to 3′. Occupancies with one strand atoms are presented in positive direction at the vertical direction and occupancies for another strand are presented in negative values.

Comparing with Na^+ ions, Rb^+ ions are more stable around the DNA.

SDFs of the cations around averaged 171d structures in the minor groove are presented in Fig. 2. It can be seen Na^+ ions are centralized distributed around ApA and TpT steps for Na180Rb20 [Fig. 2(a), 2(f)] while Rb^+ ions are released away, locating around the middle backbone of the DNA. However, neither of the ions can dominate the peripheries of the minor groove so that few ions reside there. In Na150Rb50 [Fig. 2(b), 2(g)], Na^+ ions distribute more widely but at a lower concentration than that in Na180Rb20. Rb^+ ions still cannot permeate into the minor groove. It seems that Na^+ ions dominate the A tract while Rb^+ ions concentrate around ApT steps binding to phosphates when Na^+ ions are in the majority. For Na100Rb100 [Fig. 2(c), 2(h)], it is interesting that neither of the Na^+ and Rb^+ ions can locate stably at the A tract. A few Rb^+ ions coordinate with CpG and GpC steps [Fig. 2(h)] while Na^+ ions are dispersed from the minor groove. Rb^+ ions begin to occupy the A tract in Na50Rb150 [Fig. 2(d), 2(i)], just like Na^+ ions do in Na150Rb50. Nonetheless, there are several differences in ion distributions between Na150Rb50 and Na50Rb150. In the former case, Rb^+ ions are totally dispersed from the minor groove, but in the latter case, Na^+ ions reside at the G tract. In Na20Rb180 [Fig. 2(e), 2(j)], Rb^+ ions distribute widely in the minor groove, extending from the A tract to the ApG and TpC steps, dominating the whole minor groove. It indicates that the A tract is the most favored binding position for both ions; thus it becomes the strongest competition sites. Rb^+ ions are more preferentially located in the minor groove than Na^+ ions, resulting in the stabler Rb-DNA interaction. However, both of the ions choose to reside at the G tract instead of disappearing immediately from the minor groove before entering in or after withdrawing from the A tract. The G tract is like the "springboard" for the ions permeating into the A tract in the competition.

Figure 3 shows clear difference for the RDFs and occupancies of Na^+ and Rb^+ ions relative to four electronegative sites (AN3, CO2, GN3, and TO2) in the minor groove. The maxima of RDF and occupancy appear right at the strongest cation-DNA interaction sites described above. In Fig. 3(a), Na^+ ions directly bind to the N3 of adenine (AN3) and O2 of thymine (TO2) for Na180Rb20 with the first peaks of g(r) reaching 4.9 (occupancy is 0.8) and 7.9 (1.0) at 2.5 Å, respectively. In Na150Rb50, Na^+ ions are dispersed from the adenine that the first peak of $g(r)_{AN3}$ disappears within 3 Å [Fig. 3(b)]. The strongest Na-DNA interaction site appears at TO2 with $g(r)_{TO2}$ exceeding 5 at 2.5 Å and occupancy is near 0.6. When Na^+ and Rb^+ ions are in balance, the first peaks of $g(r)_{Na^+}$ are hard to observed within 4 Å [Fig. 3(c)]. The ions contact DNA with solvent-mediated interaction in Na100Rb100. As to Na50Rb150 [Fig. 3(d)], Na^+ ions reside

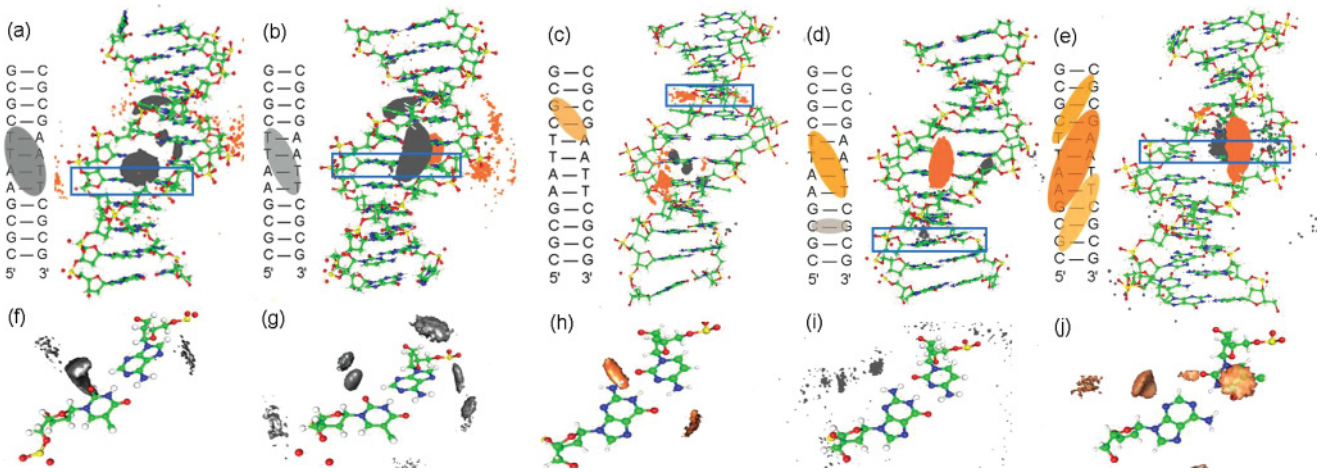

FIG. 2. (Color online) The spatial distribution functions (SDFs) of Na^+ (gray) and Rb^+ (orange or light gray) around averaged DNA secondary structures with the stereo views for Na180Rb20 (a, f), Na150Rb50 (b, g), Na100Rb100 (c, h), Na50Rb150 (d, i), and Na20Rb180 (e, j). The stereo views present global structure from (a) to (e) along the DNA helix axis toward the minor groove and the partial enlarged drawing in (f)–(j) with the minor groove at the left of the base pairs. The SDFs of ions are drawn for densities >10 particles/nm^3 in (d), and the others are drawn for densities >15 particles/nm^3.

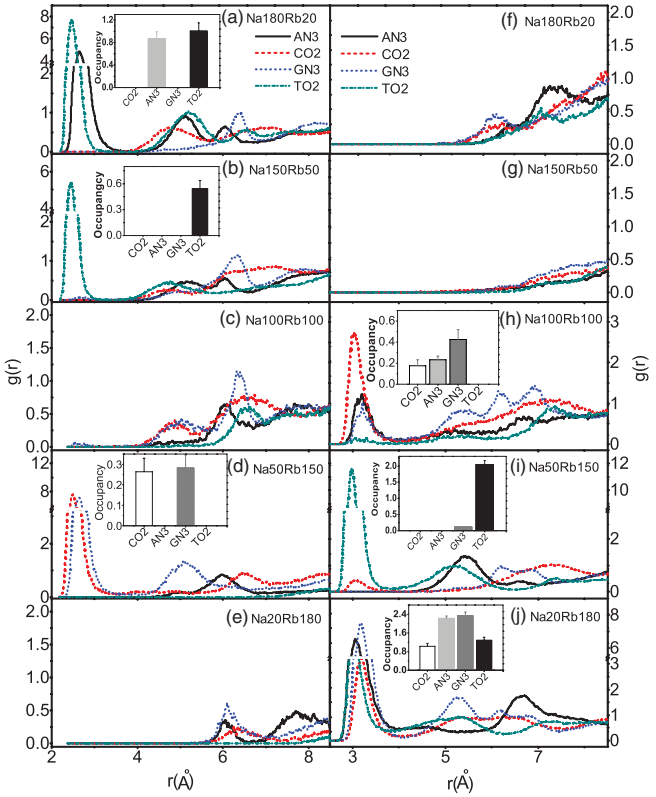

FIG. 3. (Color online) The radial distribution functions (RDFs) and the occupancies (inserts) of Na^+ (a)–(e) and Rb^+ (f)–(j) ions relative to four electronegative atoms (AN3, CO2, GN3, and TO2) in the minor groove as the ratio of Na^+ and Rb^+ ions changes from 9:1 to 1:9.

close to O2 of cytosine (CO2) and N3 of guanine (GN3). The G tract is also flavored by Na^+ ions in the competition. Moreover, a substantial amount of Na^+ ions bind to the CpG steps that the first peaks of both $g(r)_{CO2}$ and $g(r)_{GN3}$ reach 7.5 (occupancy are 0.3). In Na20Rb180, Na^+ ions are thoroughly released from the groove, and no distinct peaks appear within 5 Å [Fig. 3(e)].

Meanwhile, the values of $g(r)_{Rb^+}$ are very different from that of $g(r)_{Na^+}$. As the number of Rb^+ ions is increasing from 20 to 180, Rb^+ ions gradually permeate into the minor groove. However, Rb^+ binding is not observed in the primary layer of the "spine of hydration" in Na180Rb20 and Na150Rb50 [Fig. 3(f) and Fig. 3(g)]. As Rb^+ ions are increasing to 100 [Fig. 3(h)], the first peak of $g(r)_{CO2}$ reaches 2.5 at 3 Å and the occupancies of Rb^+ ions are highest with GN3 (0.51) and lowest with TO2 (0.05). Rb^+ ions begin to locate at the G tract. For Na50Rb150 [Fig. 3(i)], Rb^+ ions tightly bind with TO2 but are dispersed from other sites so that the first peak of $g(r)_{TO2}$ exceeds 11 (occupancy is 2.0). For Na20Rb180 [Fig. 3(j)], Rb^+ ions dominate the whole minor groove so that all of the first peaks of g(r) exceed 3 and all four occupancies reach 1.0.

To sum up, there are strong competitions between Rb^+ and Na^+ ions for residing at the A tract. When Na^+ ions are in absolute majority (Na180Rb20), they prefer binding at the A tract, and Rb^+ ions are released from the minor groove. When Na^+ ions are in a minority, Rb^+ ions dominate the whole interaction sites. The competition also happens at the G tract, especially in Na100Rb100, since both ions are withdrawn from the A tract for the strong competition. Compared with Na^+ ions, Rb^+ ions reside more at the G tract, implying the higher affinity in the minor groove, which is consistent with the experiment [28]. It can be concluded that the major competition happens at the A tract and the minor competition at the G tract. The occupancies of Rb^+ ions increase and those of Na^+ ions decrease with Rb^+ ions increasing, which is also similar with the occupancies measured in Ref. [28]. However, they found that either of the ions cannot be squeezed out completely from the minor groove. The occupancies here are also not decreases monotonically so that Na^+ ions reside around the G tract for Na50Rb150.

For the backbone-ion interaction (Fig. 2), both of the Na^+ and Rb^+ ions densely distribute at the A tract, which may be rationalized by the DNA segment electrostatic potential distribution. The ion distribution in the minor groove is also influenced by electrostatic interaction that both ions prefer to locate at the A tract, and the strongest competition happens in the middle part of the DNA. But the ionic binding to the internal DNA is determined not only by the electrostatic interaction, but also by the ionic size. In Na100Rb100, though it is harder for Rb^+ ions entering into the minor groove than Na^+ ions, Rb^+ ions can reside in the internal DNA much longer that the residence time of Rb^+ is 12.35 ps while that of Na^+ ions is just 6.54 ps at GpC steps. Rb^+ ions are trapped in the minor groove for its bigger atom radius. Moreover, comparing with the narrow A tract, the wider G tract is much easier for Rb^+ ions penetrating. Therefore, Rb^+ ions have a higher affinity at G tract in Na100Rb100. It seems that the electrostatic interaction dominate the distribution of ions that most of internal ions locate around the A tract when the number of two cations are in unbalance, while the ionic size determines the distribution of ions at the peripheries when the number of two cations are in balance.

To further check the underlying causes of the competition in the minor groove, the distributions of solvent molecule around atom AN3, CO2, GN3, and TO4 are calculated. Figure 4 presents the RDFs of the solvent molecules around these ions. It can be seen that the first peaks of $g(r)_{CO2}$ and $g(r)_{GN3}$ are slightly higher than that of $g(r)_{AN3}$ and $g(r)_{TO4}$ at 2.8 Å except RDFs in Na100Rb100. The first peak of $g(r)_{CO2}$ reaches 1.4, four times higher than that of $g(r)_{AN3}$ and $g(r)_{TO4}$ in Fig. 4(a). With the increasing of Rb^+ ions, the maximum of $g(r)_{AN3}$ is as high as that of $g(r)_{GN3}$ [Fig. 4(b)], and all of the first peaks of g(r) are around 1 in Fig. 4(c). When Rb^+ ions are in the majority, the maxima of $g(r)_{AN3}$ and $g(r)_{TO4}$ decrease, while that of $g(r)_{GN3}$ exceeds 1.2 for both Na50Rb150 and Na20Rb180 [Fig. 4(d), 4(e)].

The spine hydrations in the primary layer are dispersed from the A tract when either Na^+ or Rb^+ ions reside there. In contrast, the A tract are shield by the solvents when the ions are released out. For Na180Rb20, Na^+ ions replace the solvent molecules in the primary layer of "spine of hydration" at the A tract, leaving the G tract to the solvent molecules. As Na^+ ions are decreasing, the solvent molecules recoordinate to the primary layer, residing near the adenine for the decreasing interaction strength of Na-DNA. As for Na100Rb100, neither of the ions can stably reside at the A tract, and the solvent molecules reform the fused water hexagons. However, the ions

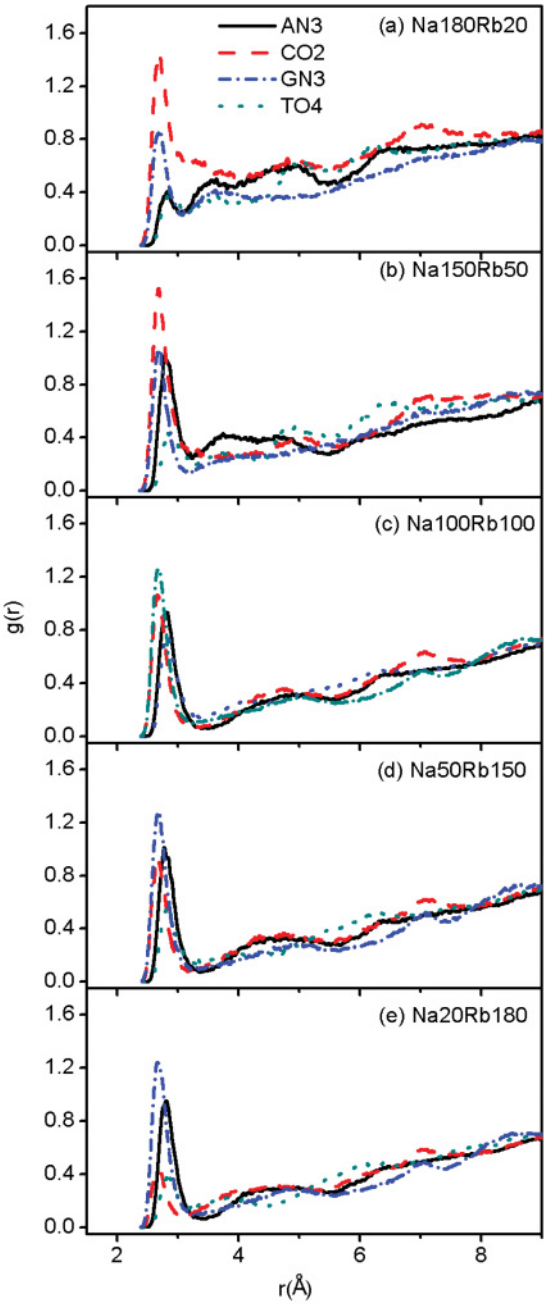

FIG. 4. (Color online) The radial distribution functions (RDFs) of the solvent molecules with four electronegative atoms (AN3, CO2, GN3, and TO2) in the minor groove for Na180Rb20 (a), Na150Rb50 (b), Na100Rb100 (c), Na50Rb150 (d), and Na20Rb180 (e).

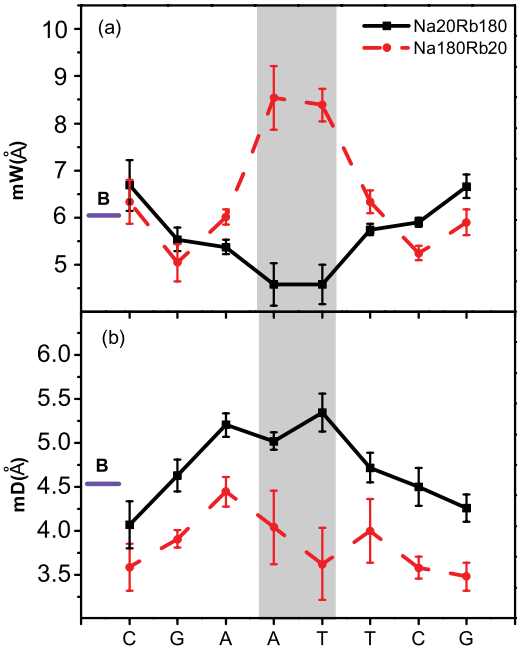

FIG. 5. (Color online) Width (a) and depth (b) of the minor groove for Na20Rb180 (solid line) and Na180Rb20 (dashed line) with violet (dark gray) short line presented the values of typical B form. The highlights show the sites where Na^+ ions influence the width and depth of the minor groove most in these two cases, respectively.

permeating into the G tract dispersed the solvent molecules out. When Rb^+ ions increase to 150, they intrude into the primary layer. Ultimately, Rb^+ ions dominate the whole minor groove while some solvent molecules still coordinate to adenine. Related to the conclusions of RDFs of ions, the strength of the hydrogen-bond decreases when the competition happens at the A tract or the G tract. Compared with the A tract, the G tract is shielded more tightly by the solvent molecules that the first peaks of $g(r)_{GN3}$ or $g(r)_{CO2}$ are higher than that of $g(r)_{AN3}$ and $g(r)_{TO4}$ in all cases except Na100Rb100. In addition, it is strange that when Na^+ ions are in majority, the solvent molecules prefer to reside close to cytosine while Rb^+ ions dominate the A tract, the hydrogen bond of guanine, and the solvent becomes the strongest.

The width and depth of minor groove (abbreviated as mW and mD, respectively) of the inner eight base pairs are influenced by ions in the competition, and we show mW and mD in Na180Rb20 and Na20Rb180, respectively, to examine the groove changing when either of the ions totally dominate the minor groove (Fig. 5). Referring to Figs. 2-4, mW and mD at the A tract are seriously influenced by the strong competition of ions. In Fig. 5(a), $mW_{Na180Rb20}$ broaden suddenly at the A tract. The widest site reaches 8.4 Å at ApT steps, which is two times wider than that of $mW_{Na20Rb180}$. In contrast, the middle part of $mW_{Na20Rb180}$ is even narrower than that at the peripheries, changing from 6.5 Å at CpG step to 4.5 Å at ApT step. In Fig. 5(b), mD reaches 5.4 Å at ApT steps for Na20Rb180, while that in Na180Rb20 is just 3.6 Å, as narrow as mD at the G tract.

Compared with the values of typical B form, Na^+ ions influence the structure of the A tract more than Rb^+ ions. It seems that Na^+ ions are capable of breaking the hexagon motif, changing the "spine of hydration," and restraining the electrostatic repulsion on DNA more than Rb^+ ions, though Rb^+ ions have higher affinity. The Na-DNA interaction changes the conformation of the A tract to a unstable state away from the typical B form when Na^+ ions dominate the minor groove. Maybe maintaining the more stable structure is also a reason that Rb^+ ions are preferentially located in the minor groove compared to Na^+ ions.

IV. CONCLUSION

A specific ion environment is crucial for DNA to perform its correct biological activity or any other novel functions. In this paper, we focus on the competition between Na^+ and Rb^+ ions and the structure changing of the minor groove. There is strong competition between Na^+ and Rb^+ ions at direct interaction sites in the minor groove. When one kind of ion is in majority, those ions are able to permeate into the primary layer of "spine of hydration" and shield the electronegative atoms in the minor groove to prevent another ion from entering in. In the competition, Rb^+ ions bind with DNA in the whole minor groove in Na20Rb180 and have higher affinity than Na^+ ions. In the meanwhile, Na^+ ions bind with DNA at the A tract and change the structure of the A tract strongly in Na180Rb20.

Our simulations show that both the electrostatic interaction and ionic size affect the competitions in the minor groove. The ionic size dominates the affinity of ions in Na100Rb100 while the electrostatic dominates the ionic affinities when the number of ion are in unbalance. The ions permeate into the minor groove from the wider G tract, which is the weaker competition site than the A tract for Na^+ and Rb^+ ions. The G tract is like the "springboard" for the ions binding to the A tract. The ions compete with each other in the whole minor groove instead of the A tract where the competition happens, and where the ions restrain the shield of the solvent molecules for the minor groove. The structure of the minor groove is changed strongly by Na^+ ions as Na^+ ions intruding into the "spine of hydration" and replacing the solvent molecules bridging the backbone. However, the structure of the minor groove changes little when Rb^+ ions dominate the minor groove, indicating the more stable characteristic for Rb^+ ions in the minor groove. Our results are consistent with the experimental phenomena and give a more clear molecular-level description of the ion-DNA interactions between two alkali-metal ions in solution.

ACKNOWLEDGMENTS

This work is supported by the National Natural Science Foundation of China under Grant Nos. 11025524 and 11161130520, the National Basic Research Program of China under Grant No. 2010CB832903, and the Sino-Ukraine Scientific Collaboration project under Grant No. CU08-04.

[1] N. C. Seeman, Nature (London) **421**, 427 (2003).
[2] K. Keren, R. S. Berman, E. Buchstab, U. Sivan, and E. Braun, Science **302**, 1380 (2003).
[3] Y. Benenson, R. Adar, T. Paz-Elizur, Z. Livneh, and E. Shapiro, Proc. Natl. Acad. Sci. USA **100**, 2191 (2003).
[4] Y. Lu and J. W. Liu, Curr. Opin. Biotechnol. **17**, 580 (2006).
[5] P. L. Privalov, A. I. Dragan1, C. Crane-Robinson, K. J. Breslauer, D. P. Remeta, and C. A. S. A. Minetti, J. Mol. Biol. **365**, 1 (2007).
[6] S. K. Sinha and S. Bandyopadhyay, J. Chem. Phys. **135**, 135101 (2011).
[7] D. Watkins, S. Mohan, G. B. Koudelka, and L. D. Williams, J. Mol. Biol. **396**, 1145 (2010).
[8] Q. Dong, E. Stellwagen, and N. C. Stellwagen, Biochem. **48**, 1047 (2009).
[9] J. Muller, Metallomics **2**, 318 (2010).
[10] W. Saenger, *Principles of Nucleic Acid Structure* (Springer, New York, 1984).
[11] T. E. Cheatham III, Curr. Opin. Struct. Biol. **14**, 360 (2004).
[12] N. Sundaresan, C. H. Suresh, T. Thomas, T. J. Thomas, and C. K. S. Pillai, Biomacromolecules **9**, 1860 (2008).
[13] S. Pal, P. K. Maiti, and B. Bagchi, J. Chem. Phys. **125**, 234903 (2006).
[14] R. Lavery, K. Zakrzewska, D. Beveridge, T. C. Bishop, D. A. Case, T. E. Cheatham III, S. Dixit, B. Jayaram, F. Lankas, C. Laughton, J. H. Maddocks, A. Michon, R. Osman, M. Orozco, A. Perez, T. Singh, N. Spackova, and J. Sponer, Nucleic Acids Res. **38**, 299 (2010).
[15] J. M. Leveritt III, C. Dibaya, S. Tesar, R. Shrestha, and A. L. Burin, J. Chem. Phys. **131**, 245102 (2009).
[16] E. Allahyarov, G. Gompper, and H. Lowen, Phys. Rev. E **69**, 041904 (2004).
[17] F. Merzel, F. Fontaine-Vive, M. R. Johnson, and G. J. Kearley, Phys. Rev. E **76**, 031917 (2007).
[18] R. Ida and G. Wu, J. Am. Chem. Soc. **130**, 3590 (2008).
[19] K. E. Furse and S. A. Corcelli, J. Phys. Chem. B **114**, 9934 (2010).
[20] K. Hibino, Y. Yoshikawa, S. Murata, T. Saito, A. A. Zinchenko, and K. Yoshikawa, Chem. Phys. Lett. **426**, 405 (2006).
[21] Y. von Hansen, R. R. Netz, and M. Hinczewski, J. Chem. Phys. **132**, 135103 (2010).
[22] N. C. Stellwagen, S. Magnusdottir, C. Gelfi, and P. G. Righetti, J. Mol. Biol. **305**, 1025 (2001).
[23] M. A. Young, B. Jayaram, and D. L. Beveridge, J. Am. Chem. Soc. **119**, 59 (1997).
[24] Y. H. Cheng, N. Korolev, and L. Nordenskiold, Nucleic Acids Res. **34**, 686 (2006).
[25] V. Tereshko, G. Minasov, and M. Egli, J. Am. Chem. Soc. **121**, 3590 (1999).
[26] K. K. Woods, L. McFail-Isom, C. C. Sines, S. B. Howerton, R. K. Stephens, and L. D. Williams, J. Am. Chem. Soc. **122**, 1546 (2000).
[27] V. P. Denisov and B. Halle, Proc. Natl. Acad. Sci. USA **97**, 629 (2000).
[28] F. C. Marincola, V. P. Denisov, and B. Halle, J. Am. Chem. Soc. **126**, 6739 (2004).
[29] A. Savelyev and G. A. Papoian, J. Am. Chem. Soc. **128**, 14506 (2006).
[30] R. Strick, P. L. Strissel, K. Gavrilov, and R. Levi-Setti, J. Cell Biol. **155**, 899 (2001).
[31] R. Ahmad, H. Arakawa, and H. A. Tajmir-Riahi, Biophys. J. **84**, 2460 (2003).
[32] M. Egli, Chem. Biol. **9**, 277 (2002).
[33] N. V. Hud and M. Polak, Curr. Opin. Struct. Biol. **22**, 293 (2001).
[34] B. I. Schweitzer, T. Mikita, G. W. Kellogg, K. H. Gardner, and G. P. Beardsley, Biochem. **33**, 11460 (1994).
[35] K. Heinzinger, Physica B **131**, 196 (1985).
[36] F. S. Zhang and R. M. Lynden-Bell, Phys. Rev. E **71**, 021502 (2005).

[37] R. M. Lynden-Bell and P. G. Debenedetti, J. Phys. Chem. B **109**, 6527 (2005).
[38] W. D. Cornell, P. Cieplak, C. I. Bayly, I. Gould, K. M. Merz Jr., D. M. Ferguson, D. C. Spellmeyer, T. Fox, J. W. Caldwell, and P. A. Kollman, J. Am. Chem. Soc. **117**, 5179 (1995).
[39] A. D. Mackerell, J. Comput. Chem. **25**, 1584 (2004).
[40] K. Toukan and A. Rahman, Phys. Rev. B **31**, 2643 (1985).
[41] A. P. Lyubartsev and A. Laaksonen, Comput. Phys. Commun. **128**, 565 (2000).
[42] R. Lohikoski, J. Timonen, and A. Laaksonen, Chem. Phys. Lett. **427**, 23 (2005).
[43] M. Tuckerman and B. J. Berne, J. Chem. Phys. **97**, 1989 (1992).
[44] D. Fincham, Mol. Simul. **13**, 1 (1994).
[45] M. P. Allen and D. J. Tildesley, *Computer Simulation of Liquids* (Oxford University, Oxford, 1987).
[46] E. Stofer and R. Lavery, Biopolymers **34**, 337 (1994).
[47] N. Boutonnet, X. W. Hui and K. Zakrzewska, Biopolymers **33**, 479 (1993).
[48] B. Gu, F. S. Zhang, Z. P. Wang, and H. Y. Zhou, Phys. Rev. Lett. **100**, 088104 (2008).
[49] X. Shen, B. Gu, S. A. Che, and F. S. Zhang, J. Chem. Phys. **135**, 034509 (2011).
[50] S. Y. Ponomarev, K. M. Thayer, and D. L. Beveridge, Proc. Natl. Acad. Sci. USA **101**, 14771 (2004).